Available online at www.sciencedirect.com
ScienceDirect
Journal of Fluorine Chemistry 128 (2007) 392–403
JOURNAL OF FLUORINE CHEMISTRY
www.elsevier.com/locate/fluor

Review

Syntheses and properties of fluorinated carbon materials

Young-Seak Lee *

Department of Fine Chemical Eng. & Applied Chemistry, BK21-E²M, Chungnam National University, Daejeon 305-764, Korea

Received 3 September 2006; received in revised form 23 November 2006; accepted 26 November 2006
Available online 1 December 2006

Abstract

In this review, the more recent topics in the field of fluorinated carbon materials are given with the emphasis on the research work presented by our group. The direct fluorination and/or oxyfluorination of various carbon materials, especially of new carbon materials, i.e. nanotubes, carbon fibers, and activated carbon fibers have been described. It has been shown that fluorination can be one of the most effective methods to modify and control physico-chemical properties of carbon materials.

Keywords: Fluorination; Oxyfluorination; Carbon nanotubes (CNTs); Carbon fibers; Activated carbon fibers (ACFs)

Contents

1. Introduction

The outstanding characteristics of F_2 molecule, e.g. extreme reactivity and oxidizing power, and the utmost electronegativity

* Tel.: +82 42 821 7007; fax: +82 42 822 6637.
E-mail address: youngslee@cnu.ac.kr.

0022-1139/$ – see front matter © 2006 Elsevier B.V. All rights reserved.
doi:10.1016/j.jfluchem.2006.11.014

of F^- ion, lead to very strong bonds between fluorine and most of the other elements of the periodical table. Therefore, fluorine, fluorinated gases and fluorinated plasmas constitute exceptional tools for modifying the surface properties of materials [1,2].

Graphite (Carbon) also reacts with fluorine gas in a wide range of the fluorination conditions. So, the chemical composition, as well as the structure of the products obtained by fluorination, is dependent on the structure and characteristics of the starting material (e.g. degree of graphitization, structural order, dimensions of the particles) and on the fluorination conditions, such as temperature, reaction time, pressure, composition of the gaseous reactants [3,4].

The diversity of carbon materials needs to be also taken into account to understand the wide range intercalation between C and F. The most important feature of C–F system is that there are two types of bonding nature, such as ionic and covalent bonding. Experimental data demonstrate that intercalated graphite with F (CF_x, $x < 0.1$), establishing C–F ionic bonds, possess extremely high electrical conductivity (close to that observed for metals, e.g. 2×10^5 S cm^{-1}) [5,6]. For high F concentrations, the transport properties of CF_x compounds decrease due to the formation of covalent bonds between the C and F atoms. At the same time, the conductivity of the material decreases and other physico-chemical property of them also changed. Therefore, in order to enlarge the application of fluorinated carbon materials not only the consideration of nature of the C–F bond but also their considerations of physical and chemical property must be taken into account.

In these sense, there are different ways to apply the direct fluorination to modify the carbon materials [7–11]. (1) An ordinary direct fluorination, i.e. treatment with elemental gaseous fluorine and/or fluorine-inert gas mixtures. This direct fluorination can be mainly used to modify surface properties of polymers [7]. In this case, hydrogen atoms are substituted for fluorine, double and conjugated bonds are saturated with fluorine. (2) Oxyfluorination, i.e. treatment of materials with fluorine–oxygen mixtures. In that case, additional >C=O, –C(O)F and –C(O)OH groups can be inserted into the structure. Usually, diluted mixtures of fluorine and nitrogen, argon, or helium are used to give functional groups on the carbon surfaces.

Numerous studies have been mainly devoted to the fluorination of graphite or graphitized carbons and to the characterization of the fluorinated compounds, which have found important practical applications [12–25]. Although several reviews on fluorinated carbon materials are available [1,3,4,25], in this review more recent topics in the field of fluorinated carbon materials are given with the emphasis on the recent research work presented by our group.

2. Effective surface modification of carbon materials by fluorination

2.1. Fluorinated carbon nanotube and applications

Since the discovery of SWCNTs [26], the nano-scale carbon tubes as a novel form of carbon materials have attracted great interest not only in science fields but also in the fields of nanotechnology applications, such as electronic devices and energy-related applications. Some intercalation and/or insertion reactions to one-dimensional type host lattice of SWCNTs have been observed [25,27–34]. In spite of the intensive researches on carbon nanotubes (CNTs), applications of CNTs to practical use of electronic and energy storage devices are still limited by the number of reasons. Carbon nanotubes are chemically inert and mechanically hard material due to their strong covalent bonds. Functionalization of a CNT wall sometimes leads to serious modification of the atomic structures. Sidewall functionalization may enhance the performance of carbon nanotubes in hydrogen storage, secondary battery, and supercapacitor.

The fluorination of single [34–41], double [42] and multi-walled [43,44] carbon nanotubes as well as graphitic fibers have only been recently developed in order to modify the structural and electronic properties of the tubular structures [5,6]. It is important to note that the electronic properties of fluorinated carbon nanotubes could in principle vary from metals to semiconductors and even to insulators [45,46] depending on the type of C–F bonding and the location of the F atoms within the carbon network. Recently, Fluorinated carbon nanotubes have proved to be useful in the new application, such as nanocomposite [39,47–50], solid lubricants [51], engineering and biomedical applications [39], and molecular electronics [52].

2.2. Surface characteristics of fluorinated SWCNTs (F-SWCNTs)

There have been recently several reports on sidewall functionalization of SWCNTs by fluorination [34,35,53–55]. This subject is of great interest for a wide variety of sidewall chemical functionalizations. Mickelson et al. has also shown in further work that F-SWCNTs are dissolved well in alcohol solvents to give long-living metastable solution [53]. Consequently, interesting routes to prepare a wide variety of functionalized nanotubes have been developing though the solution chemistry of F-SWCNTs [56]. The fluorination was reported for commercially available MWCNTs [43]. Lee et al. have investigated the change of atomic and electronic structures of F-SWCNTs powder as a function of fluorination temperature using X-ray photoelectron spectroscopy (XPS), transmission electron microscopy (TEM) and electrical resistivity measurements [34].

2.2.1. XPS and TEM observations of F-SWCNTs

Fig. 1 shows C1s XPS spectra fit spectra for the F-SWCNTs at various temperatures. The spectra of the unreacted SWCNTs ((a) in Fig. 1) give three peaks: that represent sp^2 carbon (peak 1, 284.3 eV), sp^3 carbon (peak 2, 285.0 eV) and oxygen related (carboxyl) group (peak 3, 288.5 eV). After fluorination, the intensity of sp^2 peak becomes broader and significantly reduced with increasing reaction temperatures. This sp^2 peak shape largely changes at high-temperatures above 250 °C. A variety of news peak also appear at 287.0 (peak 4, semi-ionic C–F), 288–289 (peak 6, nearly covalent C–F) and 292.0–294.05 (peak 5 and peaks 7–8, covalent CF_2, CF_3), respectively. These peaks at high binding energy side indicate the existence of various carbon

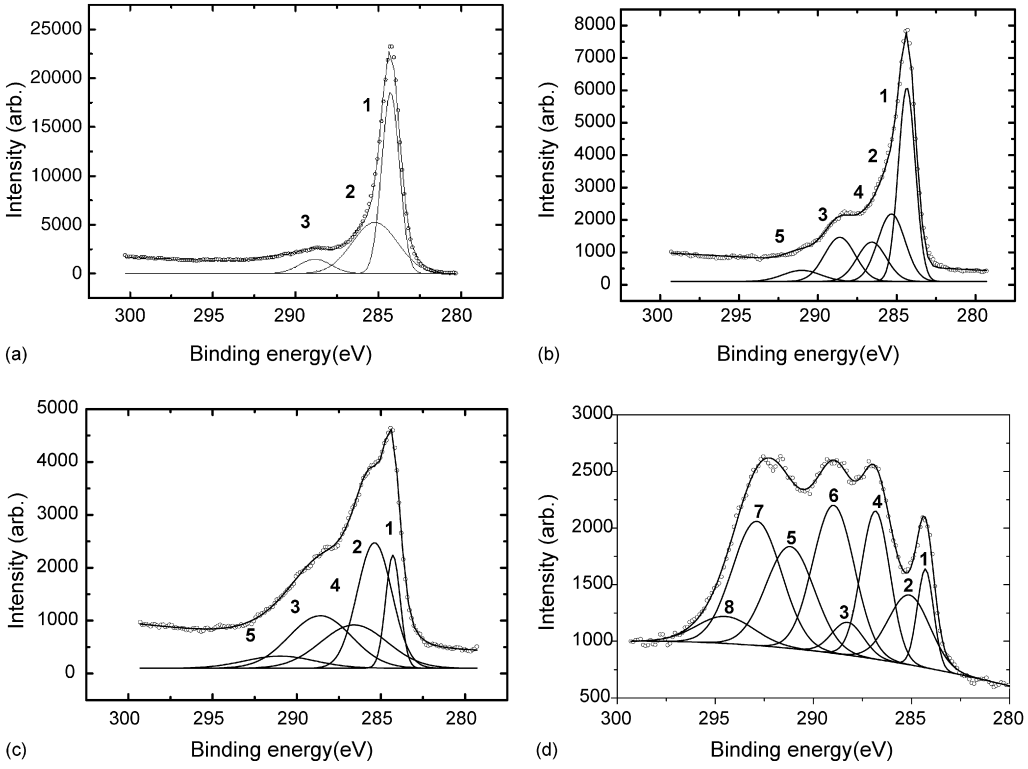

Fig. 1. C1s XPS spectra of the SWCNTS: (a) the unreacted, fluorinated at (b) 150, (c) 200 and (d) 300 °C [34].

species bonded to fluorine. The C1s peaks observed at 291.2–294.6 eV were ascribed to sp^3 hybridized carbon atoms with covalent C–F bonds, which are similar to those in the covalent compounds, graphite fluorides, $(CF)_n$ and $(C_2F)_n$ [25,34].

Fluorination was also performed for open- and closed-end SWCNTs by direct reaction of SWCNTs with elemental fluorine gas [57]. The dried SWCNT samples were fluorinated with 1 atm F_2 gas at 300, 473 and 523 K for 1 month, 5 and 5 h, respectively.

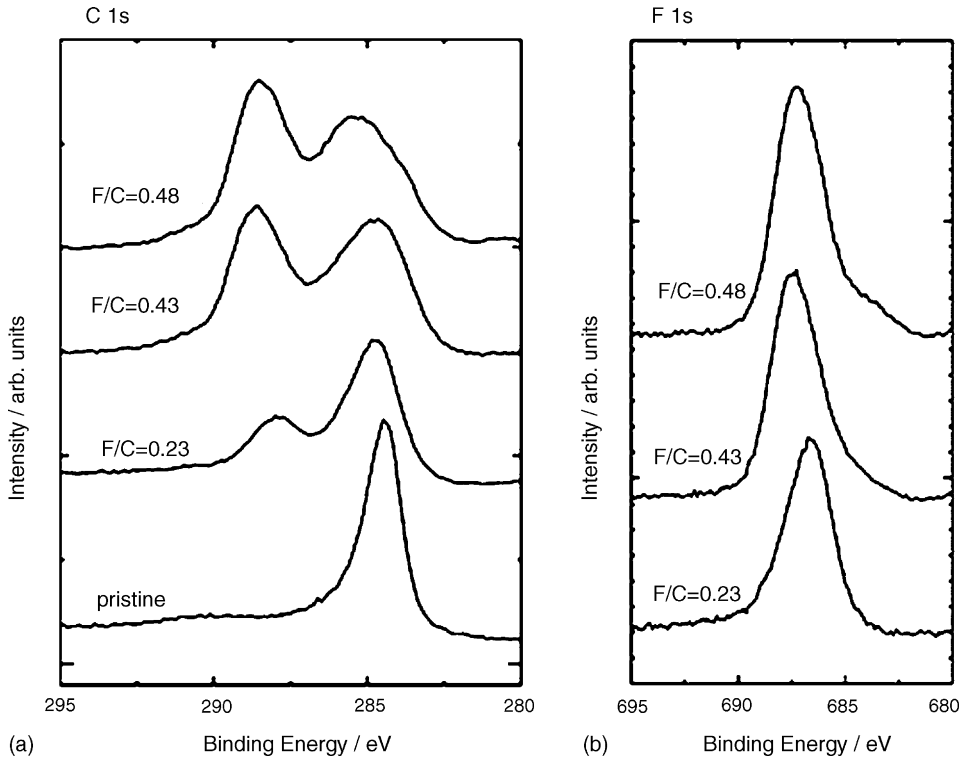

Fig. 2. Observed (a) C1s and (b) F1s XPS spectra of fluorinated o-SWCNT samples [57].

Fig. 2 shows the observed C1s and F1s XPS spectra of the fluorinated o-SWCNT samples, respectively. The fluorinated SWCNT samples have two main C1s peaks at around 288 and 285 eV, which are attributed to a carbon bound to a single F atom and a bare carbon, respectively. The C1s and F1s spectra of c-SWCNT samples (not shown) have similar features as shown by Fig. 2(a) and (b). The obtained fluorinated SWCNT samples, including o-SWCNT-F523 which has the highest fluorine content, are all black and the color change from pristine sample by fluorination was not observed by the naked eye. This is contrary to the case of fluorofullerenes where the color varies from black (C_{60}), through yellow ($C_{60}F_{36}$), to white ($C_{60}F_{48}$).

Mickelson et al. have also reported that the SWCNTs fluorinated at 500 °C are essentially all destroyed, and some MWCNT-like structures are generated [35]. Fig. 3(A) and (B) show a TEM image of the unreacted and fluorinated SWCNT at 325 °C. As can be seen from the image, the tubes remain largely intact after treatment under these conditions. Fig. 3(C) is a TEM image of SWCNTs fluorinated at 500 °C. Here it would appear that the tubes are essentially all destroyed. However, a fair number of nested tube-like graphitic structures reminiscent of MWCNTs seem to have been generated as a result of the high-temperature reaction (Fig. 3(D)).

2.2.2. FT-IR and Raman of F-SWCNTs

Infrared spectroscopy (KBr pellet method) confirmed the presence of semi-ionically and covalently bonded fluorine atoms in the same F-SWCNTs. As we can see this Fig. 4(a), a band at 1100 cm^{-1} assigned to the semi-ionic C–F bonds decreases and a band at 1210–1250 cm^{-1}, a characteristic of the C–F covalent bonds, increases with reaction temperatures. There are also typical bands that indicated due to a very small amount of moisture (OH) and CO_2 in air at about 3400 and 2350 cm^{-1}, respectively. Fig. 4(b) shows the Raman spectra of unreacted and SWCNTs fluorinated at various temperatures. The smaller peak near 200 cm^{-1} of unreacted and SWCNTs fluorinated at 150 °C is due to a characteristic-breathing mode of the SWCNTs. This breathing mode is suppressed by F-combining up to 150 °C. Each spectrum also consists of a distinctive pair of broadband at 1580 cm^{-1} (G band) and 1360 cm^{-1} (D band). The Raman peaks correspond to sp^2 and sp^3 carbon stretching modes, respectively. The I_G/I_D peak

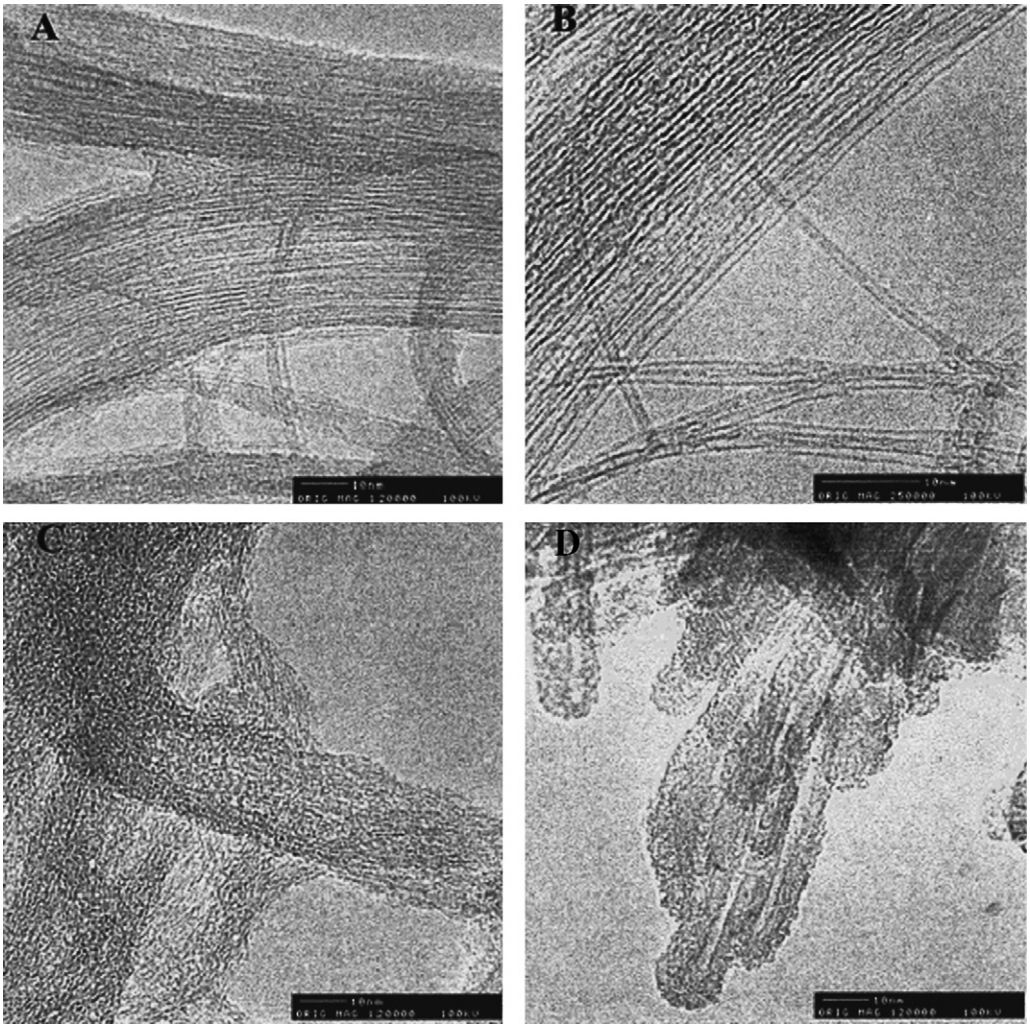

Fig. 3. (A) TEM image of unreacted SWCNTs. (B) TEM of SWCNTs after being fluorinated at 325 °C. (C) TEM of SWCNTs after being fluorinated at 500 °C. (D) TEM of SWCNTs fluorinated at 500 °C showing the formation of MWCNTs [36].

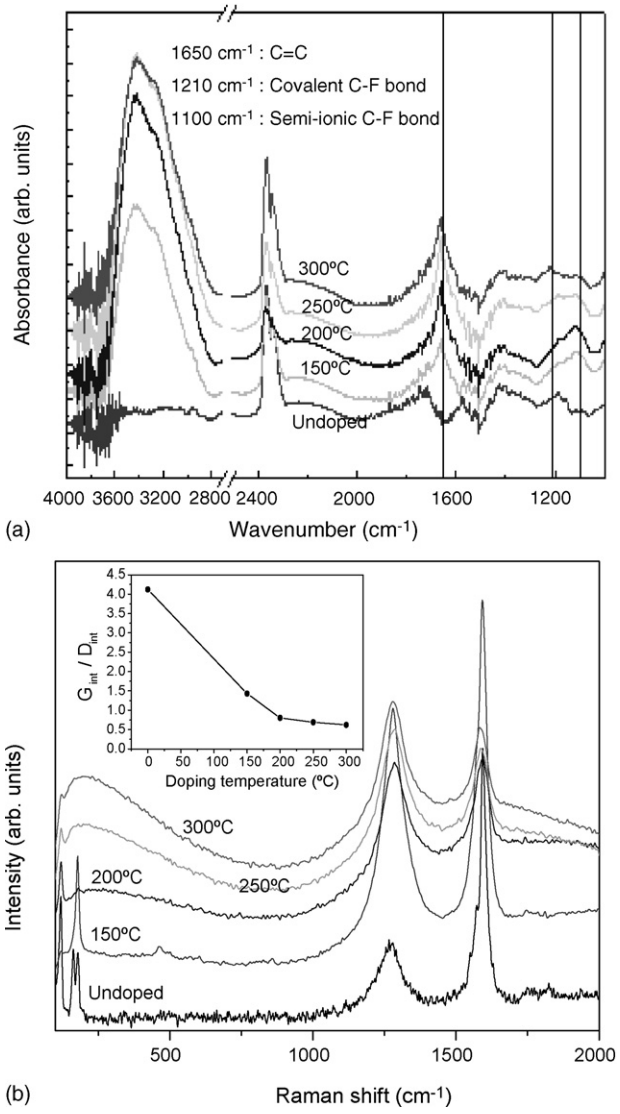

Fig. 4. (a) FT-IR data and (b) FT-Raman spectra of the SWCNTs fluorinated at various fluorination temperatures [34].

intensity ratios decrease with increasing fluorination temperature, indicating change in their structural properties in the bulk after fluorination [34].

2.3. Fluorination of ACFs

2.3.1. Microstructural properties of fluorinated ACFs (F-ACFs)

Kaneko and co-workers [58] have studied systematically the pore structures, nano-graphitic units, physical properties, and adsorptive properties of ACFs. These studies have recently been extended to F-ACFs [58–60]. Lee et al. [61] have also modified activated carbon fibers (ACFs) with high surface area and pore volume by fluorination.

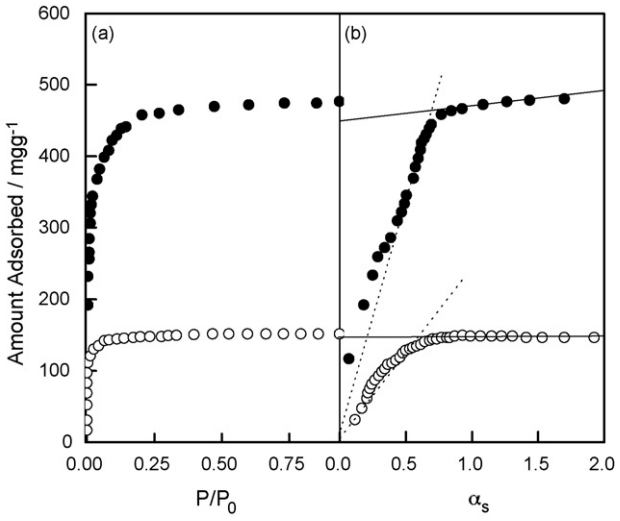

Fig. 5. Adsorption isotherms and α_s-plots of N_2 on F-ACF and ACF. Open symbols: F-ACF; filled symbols: ACF. (a) Adsorption isotherm, (b) α_s-plot [59].

Fig. 5 shows the adsorption isotherms and α_s plot of nitrogen on F-ACF and the untreated ACFs at 77 K [59]. Detailed information on the textural properties of the samples is listed in Table 1. F-ACF samples used were prepared by a direct fluorination of cellulose-derived ACFs under 1 atm of elemental fluorine gas at 100 °C. The adsorption isotherms for both samples, as seen in Fig. 5, are of type I, suggesting that both are highly microporous. The amount of nitrogen adsorbed on F-ACF is significantly smaller than on ACF owing mainly to the narrowing of micropores and the weight increase of pore walls by fluorination. The initial rise in the isotherm of F-ACF at the low relative pressure is sharper than that of ACF, suggesting that F-ACF has narrower micropores than ACF. As shown in Fig. 5 and Table 2 [61], the specific surface area and pore volume of F-ACFs were significantly decreased by fluorination.

2.3.2. Adsorptive properties of F-ACFs

Fig. 6 shows H_2O adsorption isotherm on ACF and F-ACF samples at 301 K [58]. ACF shows a pronounced adsorption hysteresis. The amount of H_2O adsorption on F-ACF is negligibly small compared with that of ACF. Kaneko and co-workers [58] found that a plausible mechanism was proposed for H_2O adsorption; water molecules in the cluster are mutually bonded with hydrogen bonds, and thereby the dispersion interaction of the effectively neutral water cluster

Table 1
Micro parameter F-ACF and ACF [59]

Sample	Surface area (m^2/g)	α_s-analysist		DR-analysis	
		Pore volume (ml/g)	Average pore width (nm)	Pore volume (ml/g)	Adsorption energy (kJmol)
F-ACF	532	0.19	0.77	0.196	15.0
ACF	1147	0.58	1.01	0.51	18.1

Table 2
Pore structure parameter of the ACFs [61]

Sample	S_{BET}[a] (m^2/g)	V_t[b](cm^3/g)	V_{mi}[c] (cm^3/g)		V_{me} N_{mi}[d]	S_{EA}[e] (m^2/g)		W_{AVP}[f] (nm)
			t-plot	α_s-plot		*t*-plot	α_s-plot	
As-received	1626.0	0.770	0.745	0.739	0.034	20.3	17.0	2.86
F1-ACF	1053.4	0.495	0.482	0.485	0.027	13.7	5.6	2.35
F2-ACF	645.7	0.400	0.391	0.378	0.023	7.8	15.0	2.22

[a] BET surface area.
[b] Total pore volume.
[c] Micropore volume.
[d] Meso/micropore volume ratio.
[e] External surface area.
[f] Average pore width.

with the carbon-walls become predominant. Accordingly, the clustered water molecule can be adsorbed in the fluorinated micropore by dispersion interaction, but the coverage of pore walls of F-ACF by water molecules at P/Po = 0.9 is only 0.035.

2.3.3. Analysis of pore size distribution (PSD) of F-ACFs

As one of the pore characteristic parameters, PSD influences the equilibrium of adsorption and transport of fluids. Other pore parameters, such as surface area and pore volume can be also obtained from information on PSD. Fig. 7 shows the pore size distributions for the fluorinated and the unreacted (as-received) ACFs [61]. Samples, F-1 and F-2, were fluorinated at room temperature with total pressure of fluorine 0.1, 0.2, respectively. All samples in this study possess primarily micropores, which, according to the IUPAC classification, have widths below 2 nm. For all samples, cumulative pore volume suggested predominance of micropores. It is also found that the total micropore volume of the surface modified ACFs decreased, as already shown in Fig. 7 and Table 2. However, average pore width (W_{AVP}) is not significantly changed by surface modification, although micropore volume is decreased. In order to comprehensively understand the effects of surface modification, especially fluorination, on the pore wall, it is necessary to determine in detail the PSD of mesopores, as well as the PSD of micropores.

3. Effective surface modification of carbon materials by oxyfluorination

To improve the carbon material–matrix interfacial interaction, it is necessary to increase the surface polarity, to create more sites for hydrogen bonding, and to improve the possibility for mechanical interlocking between the reinforcing materials and the matrix materials, in order to achieve good stress transfer from the matrix to the reinforcement [62–64]. Various surface treatment techniques have been applied to increase physical interaction. Oxyfluorination is a good candidate for this type of approach, as the numerous studies participating in the hydrogen bonding [65]. Oxyfluorinated carbon materials have also proved to be useful in the new application, such as nanocomposite [50], Ammonia removal of oxyfluorinated ACFs [66], carbon fiber composites [65,67,68].

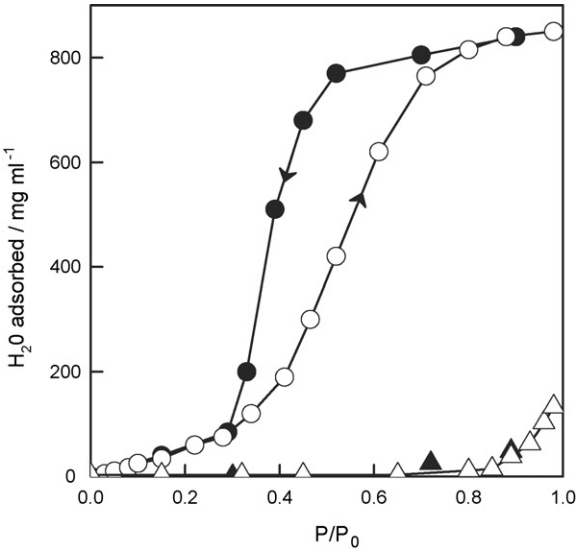

Fig. 6. Water adsorption isotherms ACF and F-ACF at 301 K; (circle) ACF; (triangle) F-ACF: open symbol : adsorption; solid symbol: desorption [58].

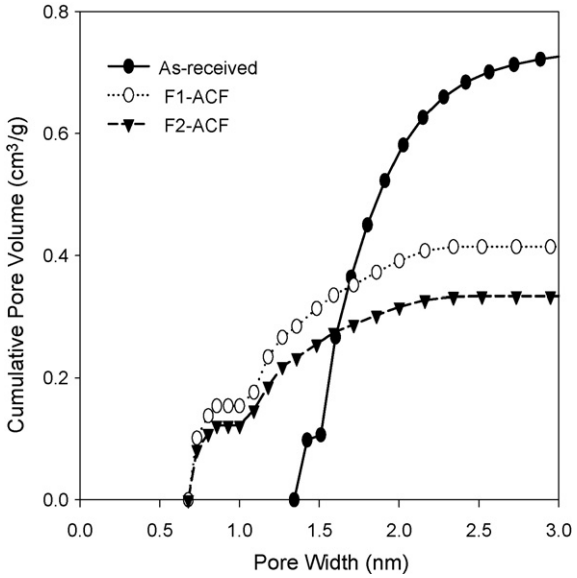

Fig. 7. Relationship between cumulative pore volume and pore width of ACFs [61].

3.1. Oxyfluorinated MWCNTs (OF-MWCNTs)

Prior to the study on SWCNT fluorination described in the previous section, the fluorination of MWCNTs was reported in 1996 by Nakajima et al. [43] and in 1997 by Hamwi et al. [44]. MWCNTs have unique atomic structure, very high aspect ratio, and extraordinary mechanical properties, making them ideal reinforcing materials in nanocomposites [27]. Thus, the properties of MWCNTs have attracted much attention from the point of view of both scientific interest and practical applications [69]. In spite of intensive research on MWCNTs, they have rarely been used as reinforcing materials in a polymeric matrix because of difficulty in achieving efficient dispersion [70,71]. This difficulty is primarily due to the non-reactive surface of MWCNTs. Therefore, the interfacial interaction between the nanotubes and the matrix is an important issue for nanocomposites.

3.2. The surface characteristics and application of OF-MWCNTs

Park et al. attempted the oxyfluorination of MWCNTs produced by chemical vapor deposition (CVD), and investigated the effect of oxyfluorination condition on surface and fracture behaviors of MWCNTs-reinforced epoxy matrix composites [50]. This is very meaningful for OF-MWCNT to apply to composite. The oxyfluorination reaction was performed with F_2, O_2, and N_2 gases in a batch reactor. The pressure was 0.2 MPa and the reaction time was 15 min at the treatment temperature.

Fig. 8 shows the FT-IR results for OF-MWCNTs. The carboxyl/ester group (C=O) at 1632 cm^2 and hydroxyl group (O–H) at 3450 cm^2 are observed for the OF-MWCNTs at above conditions. In particular, the intensity of the O–H group peak of MWCNTs exhibits the highest value at an oxyfluorination temperature of 100 °C. This result probably leads to an improvement of mechanical properties of MWCNTs-reinforced polymer matrix composites, due to the increase of specific polarity and the formation of H-bonding of the MWCNTs. Table 3 shows EDS results of OF-MWCNTs. The fluorine/oxygen contents show a maximum value in the OF-MWCNTs at 100 °C. The increasing fluorine/oxygen contents on the MWCNT surfaces may be expected to promote the specific polarity of carbon nanotubes as well as the interfacial bonding force by establishing secondary or van der Waal's forces at the interface between the reinforcement and the matrix [72].

Table 3
Composition of oxyfluorinated multi-walled carbon nanotube surfaces [50]

Specimens	C (wt.%)	O (wt.%)	F (wt.%)
Neat-MWCNTs	96.39	1.84	–
RT-MWCNTs	93.62	2.21	2.76
100-MWCNTs	92.83	2.27	3.41
200-MWCNTs	95.19	2.19	1.40
300-MWCNTs	95.72	2.08	0.74

Fig. 9 shows XRD patterns of OF-MWCNTs. For all specimens, the XRD patterns indicate the persistence of the main reflection of the original carbon nanotubes, at $d = 3.40$ Å, which could explain the lower fluorination level. The other reflections correspond unambiguously to two fluorinated nanotube phases with Ic = 6.30 and 7.46 Å. Moreover, the weak line centered at $d = 1.23$ Å can be assigned to the 110 reflection of the host lattice. These results strongly suggest that the length of the C–C bonds has remained unchanged. That is, when only the surface area is oxyfluorinated, almost no changes in the structure of graphite are observed. It may thus assume that the structure of cylindrical concentric carbon layers is preserved and that the carbon atoms retain their sp^2-hybridization.

Table 4 lists the results of fracture toughness (K_{IC}) for the composites as a function of the oxyfluorination condition. The critical stress intensity factor (K_{IC}) is also an important fracture toughness parameter, which describes the state of stress in the vicinity of the tip of a crack at fracture as a function of the specimen geometry, the crack geometry, and the applied load on the basis of linear elastic fracture mechanics [73]. As seen in Table 3, a correlation exhibits between the characteristics of the

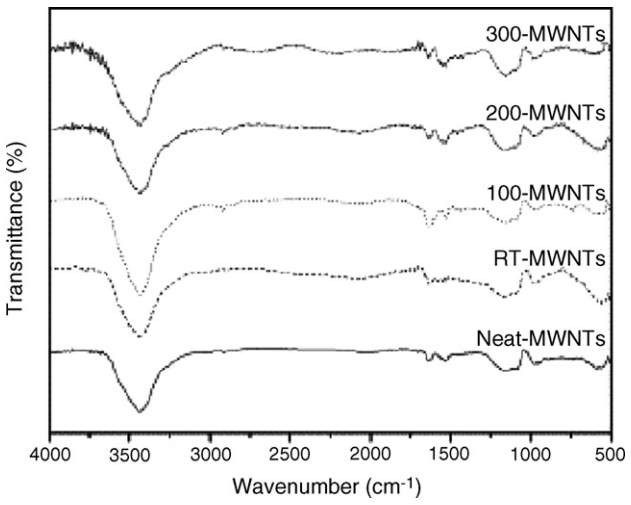

Fig. 8. FT-IR spectra of oxyfluorinated MWCNTs [50].

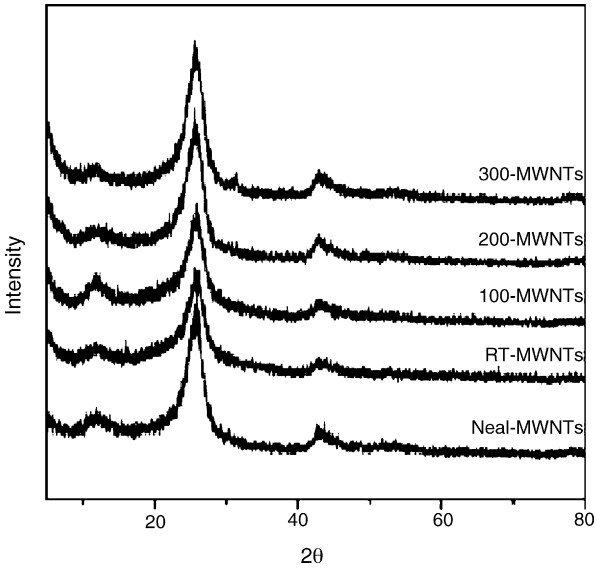

Fig. 9. Wide-angle X-ray diffraction patterns of oxyfluorinated MWCNTs [50].

Table 4
K_{IC} and impact strengths of OF-MWNTs-reinforced epoxy matrix composites [50]

Specimens	Fracture toughness (K_{IC}, MPa $m^{1/2}$)	Impact strength (kPa)
Neat-MWCNTs	2.45	21.34
RT-MWCNTs	2.63	22.23
100-MWCNTs	3.05	24.04
200-MWCNTs	2.80	22.16
300-MWCNTs	2.50	22.93

OF-MWCNT surfaces and the fracture properties of the composites. The K_{IC} values increase with increasing the polarity and oxygen functionality of the MWCNT surfaces.

Park et al. [50] have found the impact strengths of these composites increase with increasing fluorine/oxygen content. The impact strengths are important mechanical properties to evaluate the toughness of composite materials [74]. Table 4 lists the impact strength of OF-MWCNTs-reinforced composites. This result means that the fracture behavior by impact loading is often interrupted by the presence of H-bonding between the MWCNTs and the matrix resins in the composites. The H-bonding plays an important role in hindering the formation of crack growth paths, resulting in increasing impact strength of OF-MWCNTs-reinforced composites.

3.3. The surface characteristics and application of oxyfluorinated carbon fibers (OF-CFs)

Carbon fibers (CFs) are widely used and of technological importance as reinforcing materials in high performance composites materials. They combine a high stress factor and strength with a low density, which has led to their increasing use in high performance construction materials. Considerable effort is being expanded to modify the properties of these fibers [75,76]. An alternative technique to increase the surface polarity of carbon is mild fluorination using elemental fluorine [77]. Several studies on fluorinated carbon fibers were reported [78–82].

Lee and Lee [83] and Lee and co-workers [84] investigated in detail oxyfluorinated PAN-based carbon fibers at room temperature using fluorine–oxygen mixtures, and the influence of oxyfluorination on various properties, such as wettability, surface polarity, surface free energy, conductivity and tensile strength.

3.3.1. Surface composition and chemical bonds of OF-CFs

In Table 5 are shown the XPS C1s, F1s and O1s binding energies, and relative amounts of C, F and O of oxyfluorinated carbon fiber [83]. The oxyfluorination conditions for PAN-based carbon fibers are given in Table 6. The percentage of functional groups (C–OH, C=O, COOH) on these samples were calculated from the areas of deconvoluted C1s peaks. The surface composition calculated from the peak areas of XPS is also summarized in Table 5.

As shown in Fig. 10(a), deconvolution of the C1s spectra of as-received PAN-based carbon fibers (S-1 in Fig. 10) gives three peaks : that represent graphitic carbon (peak 1, 284.41 eV), phenolic carbon, hydroxyl, carbonyl groups (peak 2, 285.90 eV), and carboxyl group (peak 3, 288.05 eV). After oxyfluorination, the relative content of graphitic carbon (peak 1) is significantly decreased (as shown in Table 5) and

Table 5
C1s, F1s and O1s binding energies, relative amounts of C, F and O in each spectrum before and after oxyfluorination of CFs [83]

Sample	Binding energy (eV); relative amount (%)				Assignment of the components
	S-1	S-2	S-3	S-4	
C1s	284.41; 55	284.28; 40	284.28; 38	284.40; 45	Graphitic C
	285.90; 25	285.71; 44	285.61; 44	285.80; 39	COH, C=O
	288.05; 20	288.16; 5	288.17; 6	288.11; 7	HO–C=O
		289.48; 6	289.65; 6	289.24; 4	Semicovalent CF
		290.33; 5	290.26; 6	290.37; 5	Covalent CF
F1s	–	686.90; 86	686.84; 85	686.70; 20	Semicovalent CF
	–	688.39; 14	688.39; 15	688.31; 80	Covalent CF
O1s	532.07; 54	531.94; 43	531.93; 41	532.31; 52	C=O
	533.72; 46	533.39; 57	533.34; 59	533.73; 48	COH
Composition	$C_{55}O_{45}$	$C_{40}O_{49}F_{11}$	$C_{38}O_{50}F_{12}$	$C_{45}O_{46}F_{9}$	-

Table 6
Oxyfluorination conditions of PAN-based carbon fibers used for XPS analysis

Fiber notation	Experimental conditions		
	Total pressure (kPa)	O_2 mole fraction	Oxyfluorination time (min)
S-1	Untreated carbon fibers		
S-2	5	0.5	30
S-3	5	0.5	60
S-4	80	0.5	30

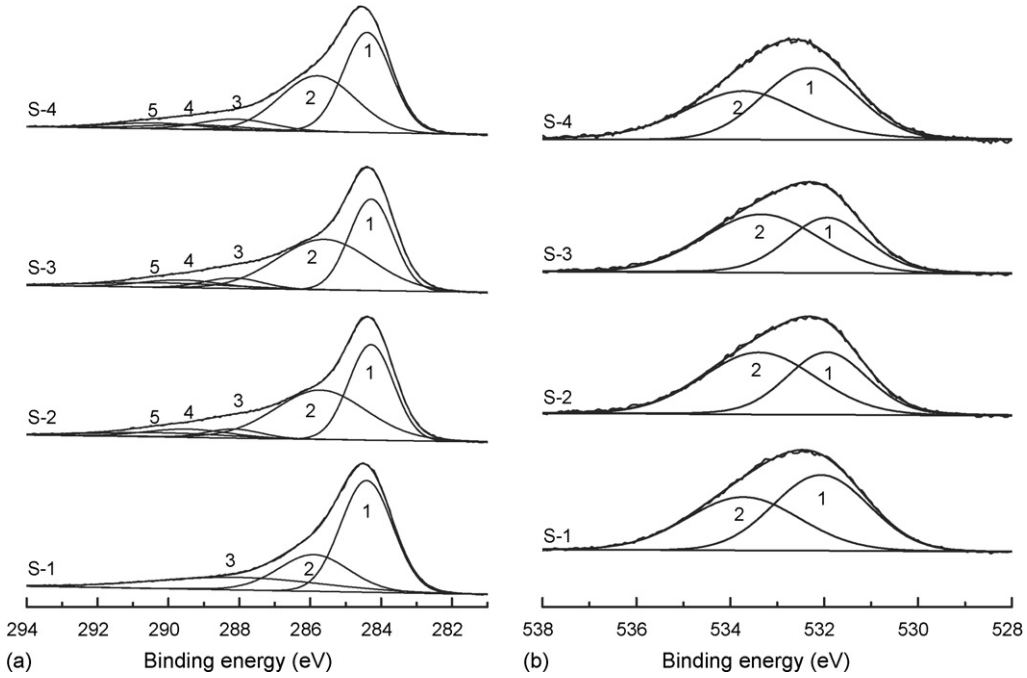

Fig. 10. C1s XPS (a) and O1s XPS (b) spectra of as-received (S-1), and oxyfluorinated CFs (S-2, S-3, S-4) [83].

additional peaks 4 and 5 appear at 289.5 (peak 4, semi-covalent C–F) and 290.3 eV (peak 5, covalent C–F), respectively. Table 5 indicated that the oxyfluorination causes increase in the amount of oxygen, while the amount of oxygen is strongly reduced by direct fluorination [10].

Fig. 10(b) shows the O1s spectra fitted to two component peaks. Peak 1 (531.93–532.31 eV) corresponds to C=O groups (ketone, lactone, carbonyl) and peak 2 (5333.34–533.73 eV) to C–OH and/or C–O–C groups. The C=O contribution to the O1s spectra significantly decreases from 54% (as-received fiber) to 41–43% after oxyfluorination at total pressure of 5 kPa. In these cases, the peak 1/peak2 area ratios for as-received fiber (S-1) and oxyfluorinated fibers (S-2 and S-3) are >1 and <1, respectively.

3.3.2. Effect of total pressure on the wettability of OF-CFs

The contact angles of water and diiodomethane were measured and surface free energies of OF-CFs were calculated. These results are presented in Table 7. The contact angles of water on carbon fibers indicated that the oxyfluorination at a total pressure of 5 kPa increases the wettability of carbon fibers, but the wettability gradually decreases with increasing total pressure. With increasing total pressure for oxyfluorination, the contact angles of water remarkably increase again until its value is slightly higher than that of the untreated carbon fiber, while the contact angle of diiodomethane is unchanged. The low total pressure and introduction of oxygen might explain the increased wettability. This behavior may be caused by formation of hydrophilic C–O and semi-covalent C–F bond. At higher total pressures, the OF-CFs demonstrated high contact angles of water, that is, high hydrophobicity. The polarity was initially increased and then gradually decreased with total pressure of reaction gases [83].

Table 7
Surface free energies and polarity of oxyfluorinated PAN-based carbon fibers as a function of total pressure [83]

Total pressure (kPa)	γ^p (mJ/m^2)	γ^d (mJ/m^2)	γ (mJ/m^2)	$X^p = \gamma^p/\gamma$
–	0.0	21.4	21.4	0.00
5	41.4	11.1	52.5	0.79
10	28.7	14.8	43.5	0.66
20	8.1	18.8	26.9	0.30
40	0.0	18.5	18.5	0.00
80	0.0	17.5	17.5	0.00

3.3.3. XRD analysis of OF-CFs

Park et al. [67] have investigated XRD of oxyfluorinated CFs. Fig. 11 shows the XRD patterns of fluorinated and

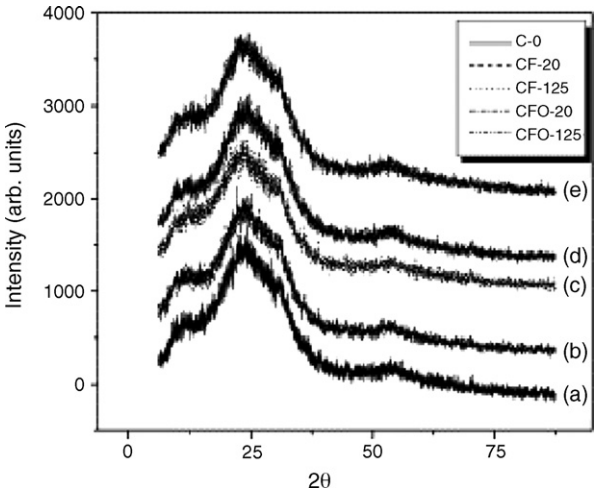

Fig. 11. X-ray diffraction patterns of the fluorinated CFs. (a) C-0, (b) CF-20, (c) CF-125, (d) CFO-20, (e) CFO-125 [67].

Table 8
2θ values and calculated interlayer distances of the fluorinated PAN-based carbon fibers [67]

Specimens	$\Delta\theta_{1/2}$(°)	2θ(°)	d_2 (Å)
C-0	2.41	25.13	3.53
CF-20	2.79	25.34	3.52
CF-125	2.85	25.35	3.55
CFO-20	3.03	25.51	3.49
CFO-125	3.10	25.53	3.51

oxyfluorinated carbon fibers. When only the surface area is fluorinated, almost no change in the (0 0 2) diffraction line of graphite is observed. No increase in the interlayer distance is found, as shown in Table 8. Assuming that the carbon fibers are made up of onion skin and ordered graphite layers [85], the graphitic framework is relatively rigid and may resist intercalation or bulk fluorination when mild fluorination conditions (CF-20 and CF-125) are applied. All of the fluorinated fibers have the same interlayer distance within the error limits (the peak shape allows an accuracy of $\Delta\theta_{1/2} = \pm 0.4°$). The half-width of the peak increases and the peak height strongly decreases after fluorination of the fiber materials. The slight change of morphology of fluorinated fibers is not due to the formation of covalent carbon fluoride, but to the partial formation of stage 1 C_xF with a physical C–F bonding at 688.1 eV [86].

3.3.4. Mechanical properties of OF-CFs

Fig. 12 shows the tensile strength and Young's modulus of the single filament carbon fibers according to the treatment conditions. Tensile strength as well as Young's modulus increase, and their maximum values show after F_2/O_2 mixture treatment (CFO-125) at 125 °C. The increase in tensile strength and Young's modulus is 36 and 32%, respectively. The fluorination probably increases the surface polarity of the fibers and introduces the active sites for hydrogen bonding and van der Waal's force between the fiber and the surrounding polymer matrix, which imply that an intercalation-type interaction can be formed between the fiber and the polymer matrix [87]. Interlaminar shear strength (ILSS) of epoxy composite is also improved when using the OF-CFs as reinforcement [67].

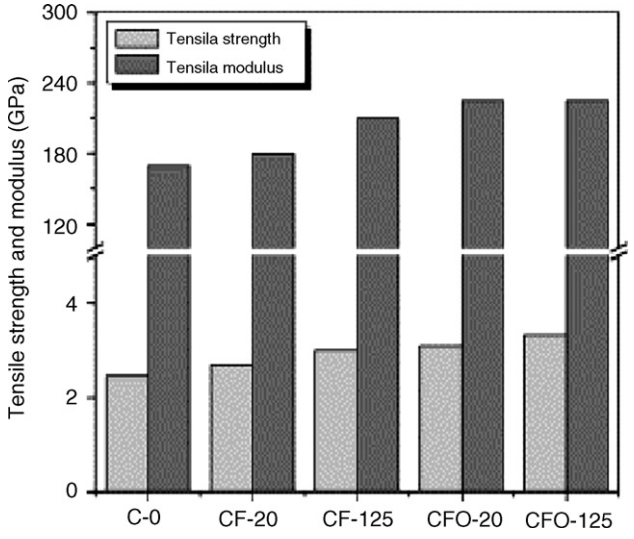

Fig. 12. Tensile strength and Young's modulus of the fluorinated CFs [67].

3.4. Oxyfluorinated activated carbon fiber (OF-ACFs)

ACFs have been widely recognized as a promising material for removing and preventing odor or fumes. ACFs consist of a three-dimensional random network of nano-graphitic units which gives considerably uniform slit-shaped micropores and characteristic adsorption properties. Oxy-fluorination of ACFs effectively modifies their electronic and structural properties. This suggests the effectiveness of fluorination for the preparation of ACF-derived carbon which would bring about further functionality related to potential applications [61].

3.4.1. Ammonia removal of OF-ACFs

Ammonia gas is considered a high health hazard because it is corrosive to the skin, eyes, and lungs. Prolonged contact at concentrations greater than 300 ppm can cause permanent injury or death. However, general ACFs do not have enough adsorption capacity for ammonia because ACFs usually posses a nonpolar surface due to manufacturing conditions at high-temperatures, which is a disadvantage for some applications because of a poor interaction with some polar adsorbates. Park and Kim have reported that OF-ACFs could enhance the capacity of ammonia gas removal [66]. The ammonia-removal capacity of the ACFs before and after oxyfluorination is shown in Fig. 13. The capacities of all OF-ACFs are at a higher level than that of the as-received sample, and it increase with the treatment time. It can be seen that the ammonia-adsorption ability of the as-received sample is sharply decreased within a few hours, and it reaches about 950 ppm after 10 h. However, FO-5 can withstand 2 h, and FO-10 can even show a breakthrough at 4.5 h of the reaction time. It is proved that newly introduced surface functional groups containing carbon–

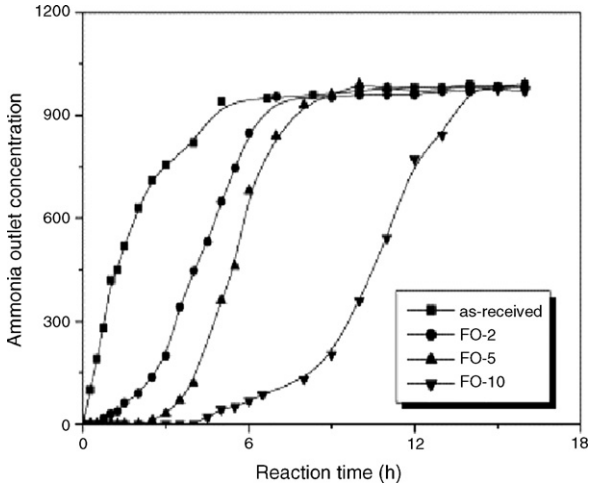

Fig. 13. Ammonia gas removal of the OF-ACFs as a function of treatment time [66].

oxygen or–fluorine complexes on ACF surfaces play a major role in improving ammonia removal. Thus, oxyfluorination can be tentatively proposed as a suitable method for ammonia gas removal of a basic nature [66].

4. Conclusion

Fluorinated carbon materials have many valuable characteristics and applications. Nevertheless, in order to enlarge much more application of fluorinated carbon materials, many efforts are need to be taken into account not only the consideration of nature of the C–F bond but also their considerations of chemical and physical property. With the development of their synthesis and applications of fluorinated carbon materials, it is certain that even more exiting and interesting results are waiting in these fields.

Acknowledgements

This research (review paper) was performed for the Hydrogen Energy R&D Center, one of the 21st Century Frontier R&D Program, funded by the Ministry of Science and Technology of Korea.

References

[1] T. Nakajima, in: T. Nakajima (Ed.), Fluorine–Carbon and Fluoride–Carbon Materials: Chemistry, Physics and Applications, Marcel Dekker, New York, NY, 1995.
[2] A. Tressaud, E. Durand, C. Labrugère, J. Fluorine Chem. 125 (2004) 1639–1648.
[3] T. Nakajima, N. Watanabe, Graphite Fluorides and Carbon-Fluorine Compounds, Boca Raton, CRC Press, 1990.
[4] N. Watanabe, T. Nakajima, H. Touhara, Graphite Fluorides, 56th ed., Elsevier, Amsterdam, 1988.
[5] L. Piraux, V. Bayot, J.P. Issi, M.S. Dresselhaus, M. Endo, T. Nakajima, Phys. Rev. B41 (1990) 4961–4969.
[6] T. Nakajima, N. Watanabe, I. Kameda, M. Endo, Carbon 24 (1986) 343–351.
[7] A.P. Kharitonov, R. Taege, G. Ferrier, V.V. Teplyakov, D.A. Syrtsova, G.-H. Koops, J. Fluorine Chem. 126 (2005) 251–263.
[8] P.A.B. Carstens, S.A. Marais, C.J. Thompson, J. Fluorine Chem. 104 (2000) 97–107.
[9] A.P. Kharitonov, J. Fluorine Chem. 103 (2000) 123–127.
[10] J.P. Hobbs, P.B. Henderson, M.R. Pascolini, J. Fluorine Chem. 104 (2000) 87–95.
[11] V.G. Nazarov, F.A. Makhmutov, Colloid J. 62 (2000) 594–599.
[12] T. Nakajima, V. Gupta, Y. Ohzawa, M. Koh, R.N. Singh, A. Tressaud, E. Durand, J. Power Sources 104 (2002) 108–114.
[13] J. Giraudet, M. Dubois, J. Inacio, A. Hamwi, Carbon 41 (2003) 453–463.
[14] T. Nakajima, V. Gupta, Y. Ohzawa, H. Iwata, A. Tressaud, E. Durand, Mol. Cryst. Liquid Cryst. 388 (2002) 103–108.
[15] T. Nakajima, V. Gupta, Y. Ohzawa, H. Iwata, A. Tressaud, E. Durand, J. Fluorine Chem. 114 (2002) 209–214.
[16] T. Nakajima, J. Li, K. Naga, K. Yoneshima, T. Nakai, Y. Ohzawa, J. Power Sources 133 (2004) 243–251.
[17] T. Fukutsuka, S. Hasegawa, Y. Matsuo, Y. Sugie, T. Abe, Z. Ogumi, J. Power Sources 146 (2005) 151–155.
[18] J. Li, K. Naga, Y. Ohzawa, T. Nakajima, A.P. Shames, A.I. Panich, J. Fluorine Chem. 126 (2005) 265–273.
[19] J. Li, Y. Ohzawa, T. Nakajima, H. Iwata, J. Fluorine Chem. 126 (2005) 1028–1035.
[20] H. Groult, T. Nakajima, L. Perrigaud, Y. Ohzawa, H. Yashiro, S. Komaba, N. Kumagai, J. Fluorine Chem. 126 (2005) 1111–1116.
[21] C. Delabarre, M. Dubois, J. Giraudet, K. Guérin, A. Hamwi, Carbon 44 (2006) 2543–2548.
[22] C. Delabarre, M. Dubois, K. Guérin, Z. Fawal, A. Hamwi, J. Phys. Chem. Solids 67 (2006) 1157–1161.
[23] K. Naga, Y. Ohzawa, T. Nakajima, Electrochim. Acta 51 (2006) 4003–4010.
[24] K. Matsumoto, J. Li, Y. Ohzawa, T. Nakajima, Z. Mazej, B. Žemva, J. Fluorine Chem. 127 (2006) 1383–1389.
[25] H. Touhara, F. Okino, Carbon 38 (2000) 241–267.
[26] S. Iijima, Nature 354 (1991) 56–58.
[27] E.T. Thostenson, Z. Ren, T.W. Chow, Compos. Sci. Technol. 61 (2001) 1899–1912.
[28] R.S. Lee, H.J. Kim, J.E. Fischer, A. Thess, R.E. Smalley, Nature 64 (1988) 6464–6468.
[29] S. Suzuki, M. Tomita, J. Appl. Phys. 79 (1996) 3739–3743.
[30] A.C. Dillon, K.M. Jones, T.A. Bekkedahl, C.H. Kiang, D.S. Bethune, M.J. Heben, Nature 386 (1997) 377–379.
[31] R.S. Lee, H.J. Kim, J.E. Fischer, A. Thess, R.E. Smalley, J. Appl. Phys. 388 (1997) 255–257.
[32] D.E. Sklovsky, H. Gaucher, G.N. Bondarenko, S. Menu, F. Beguin, S. Bonnamy, J. Conard, V.A. Nalimova, Mol. Cryst. Liquid Cryst. 310 (1998) 165–172.
[33] A.G. Rinzler, J. Liu, H. Dai, P. Nikolaev, C.B. Huffman, F.J. Rodriguez-Macias, P.J. Boul, A.H. Lu, D. Heymann, D.T. Colbert, R.S. Lee, J.E. Fischer, A.M. Rao, P.C. Eklund, R.E. Smalley, Appl. Phys. Sect. A Mater. Sci. Process. 67 (1998) 29–38.
[34] Y.S. Lee, T.H. Cho, B.K. Lee, J.S. Rho, K.H. An, Y.H. Lee, J. Fluorine Chem. 120 (2003) 99–104.
[35] E.T. Mickelson, C.B. Huffman, A.G. Rinzler, R.E. Smalley, R.H. Hauge, J.L. Margrave, Chem. Phys. Lett. 296 (1998) 188–194.
[36] K.F. Kelly, I.W. Chiang, E.T. Mickelson, R.H. Hauge, J.L. Margrave, X. Wang, G.E. Scuseria, C. Radloff, N.J. Halas, Chem. Phys. Lett. 313 (1999) 445–450.
[37] T. Hayashi, M. Terrones, C. Scheu, Y.A. Kim, M. Ruhle, T. Nakajima, M. Endo, Nano Lett. 2 (2002) 491–496.
[38] H. Miyagawa, L.T. Drzal, Polymer 45 (2004) 5163–5170.
[39] V.N. Khabashesku, J.L. Margrave, E.V. Barrera, Diamond Relat. Mater. 14 (2005) 859–866.
[40] L. Valentini, J. Macan, I. Armentano, F. Mengoni, J.M. Kenny, Carbon 44 (2006) 2196–2201.
[41] U. Dettlaff-Weglikowska, V. Skakalova, J. Meyer, J. Cech, B.G. Mueller, S. Roth, Curr. Appl. Phys. 7 (2007) 42–46.
[42] H. Muramatsu, Y.A. Kim, T. Hayashi, M. Endo, A. Yonemoto, H. Arikai, F. Okino, H. Tohara, Chem. Commun. (2005) 2002–2004.
[43] T. Nakajima, S. Kasamatsu, Y. Matsuo, Eur. J. Solid State Inorg. Chem. 33 (1996) 831–840.
[44] A. Hamwi, H. Alvergnat, S. Bonnamy, F. Beguin, Carbon 35 (1997) 723–728.
[45] G. Seifert, T. Kohler, T. Frauenheim, Appl. Phys. Lett. 77 (2000) 1313–1315.
[46] K.N. Kudin, H.F. Bettinger, G.E. Scuseria, Phys. Rev. B63 (2001) 45413–45421.
[47] H. Miyagawa, M.J. Rich, L.T. Drzal, Thermochim. Acta 442 (2006) 67–73.
[48] F.J. Owens, Mater. Lett. 59 (2005) 3720–3723.
[49] H.W. Goh, S.H. Goh, G.Q. Xu, K.P. Pramoda, W.D. Zhang, Chem. Phys. Lett. 379 (2003) 236–241.
[50] S.J. Park, H.J. Jeong, C.W. Nah, Mater. Sci. Eng. A385 (2004) 13–16.
[51] R.L. Vander Wal, K. Miyoshi, K.W. Street, A.J. Tomasek, H. Peng, Y. Liu, J.L. Margrave, V.N. Khabashesku, Wear 259 (2005) 738–743.
[52] N.O.V. Plank, R. Cheung, Microelectron. Eng. 73–74 (2004) 578–582.
[53] E.T. Mickelson, I.W. Chiang, J.L. Zimmerman, P.J. Boul, J. Lozano, J. Liu, R.E. Smalley, R.H. Hauge, J.L. Margrave, J. Phys. Chem. B 103 (1999) 4318–4322.
[54] N.G. Lebedev, I.V. Zaporotskova, L.A. Chernozatonskii, Microelectron. Eng. 69 (2003) 511–518.

[55] N.O.V. Plank, L.D. Jiang, R. Cheung, Appl. Phys. Lett. 83 (2003) 2426–2428.
[56] K.F. Kelly, I.W. Chiang, E.T. Mickelson, R.H. Hauge, J.L. Margrave, X. Wang, G.E. Scuseria, C. Radolff, N.J. Halas, J. Phys. Chem. B103 (1999) 440–445.
[57] S. Kawasaki, K. Komatsu, F. Okino, H. Touhara, H. Kataura, Phys. Chem. Chem. Phys. 6 (2004) 1769–1772.
[58] G. Li, K. Kaneko, S. Ozeki, F. Okino, R. Ishikawa, M. Kanda, H. Touhara, Langmuir 11 (1995) 716–717.
[59] N. Setoyama, G. Li, K. Kaneko, F. Okino, R. Ishikawa, M. Kanda, H. Touhara, Adsorption 2 (1996) 293–297.
[60] G. Li, K. Kaneko, S. Ozeki, F. Okino, H. Touhara, J. Colloid Interface Sci. 172 (1995) 539–540.
[61] Y.S. Lee, Y.H. Kim, J.S. Hong, J.K. Suh, G.J. Cho, Catal. Today, in press.
[62] J.P. Salvetat, G.D.A. Briggs, J.M. Bonard, R.R. Bacsa, A.J. Kulik, T. Stöckli, N.A. Burnham, L. Forró, Phys. Rev. Lett. 82 (1999) 944–947.
[63] P.M. Ajayan, L.S. Schadler, C. Giannaris, A. Rubio, Adv. Mater. 12 (2000) 750–753.
[64] S.J. Park, M.K. Seo, T.J. Ma, D.R. Lee, J. Colloid Interface Sci. 252 (2002) 249–255.
[65] S.J. Park, M.K. Seo, J.R. Lee, J. Colloid Interface Sci. 268 (2003) 127–132.
[66] S.J. Park, B.J. Kim, J. Colloid Interface Sci. 291 (2005) 597–599.
[67] S.J. Park, M.K. Seo, Y.S. Lee, Carbon 41 (2003) 723–730.
[68] S.J. Park, M.K. Seo, Y.S. Lee, Carbon Sci. 4 (2003) 69–73.
[69] Z. Ounaies, C. Park, K.E. Wise, E.J. Siochi, J.S. Harrison, Compos. Sci. Technol. 63 (2003) 1637–1646.
[70] M.S.P. Shaffer, A.H. Windle, Adv. Mater. 11 (1999) 937–941.
[71] E. Kymakis, I. Alexandou, G.A.J. Amaratunga, Synth. Met. 127 (2002) 59–62.
[72] S.J. Park, Interfacial Forces and Field: Theory and Application, Marcel Dekker, New York, 1999.
[73] S.J. Park, M.H. Kim, J.R. Lee, S. Choi, J. Colloid Interface Sci. 228 (2000) 287–291.
[74] O. Allix, M. Dommanget, M. Gratton, P.L. Héreil, Compos. Sci. Technol. 61 (2001) 409–415.
[75] W. Ruland, Adv. Mater. 2 (1990) 528–536.
[76] F.J. Toit, R.D. Sanderson, J. Fluorine Chem. 98 (1999) 107–114.
[77] Y.B. Chong, H. Ohara, J. Fluorine Chem. 57 (1997) 169–175.
[78] A. Bismark, R. Tahhan, J. Springer, A. Schulz, T.M. Klapotke, H. Zell, W. Michaeli, J. Fluorine Chem. 84 (1997) 127–134.
[79] R.B. Mathur, V. Gupta, O.P. Bahl, A. Tressaud, S. Flandrois, Synth. Met. 114 (2000) 197–200.
[80] V. Gupta, R.B. Mathur, O.P. Bahl, A. Tressaud, S. Flandrois, Synth. Met. 73 (1995) 69–75.
[81] L. Fischer, U. Siemann, W. Ruland, Colloid Polym. Sci. 261 (1983) 744–749.
[82] M. Zayat, D. Davidov, H. Selig, Carbon 32 (1994) 485–491.
[83] Y.S. Lee, B.K. Lee, Carbon 40 (2002) 2461–2468.
[84] I.S. Lim, S.H. Yoo, I.N. Park, Y.S. Lee, Carbon Sci. 5 (2004) 12–17.
[85] T. Isshiki, F. Okino, Y. Hattori, S. Kawasaki, H. Touhara, Carbon 35 (1997) 716–723.
[86] D.K. Padma, R.N. Singh, J. Fluorine Chem. 54 (1991) 133–138.
[87] G. Krekel, K.J. Huttinger, W.P. Hoffman, D.S. Silver, J. Mater. Sci. 29 (1994) 2968–2980.